A Linear Multi-Objective Operation Model for Smart Distribution Systems Coordinating Tap-Changers, Photovoltaics and Battery Energy Storage

Naser Hashemipour, Taher Niknam
SUT, Shiraz, Iran
n.hashemipour@sutech.ac.ir; niknam@sutech.ac.ir

Jamshid Aghaei, Hossein Farahmand, Magnus Korpås
NTNU, Trondheim, Norway
aghaei@ntnu.no; hossein.farahmand@ntnu.no; magnus.korpås@ntnu.no

Miadreza Shafie-khah, Gerardo J. Osório
C-MAST/UBI, Covilha, Portugal
miadreza@ubi.pt; gjosilva@gmail.com

João P. S. Catalão
INESC TEC and FEUP, Porto, C-MAST/UBI, Covilha, and INESC-ID/IST-UL, Lisbon, Portugal
catalao@fe.up.pt

***Abstract*—Uncontrolled operation of distributed generation (DG) can cause interference with the operation of other equipment such as tap-changers, and non-optimal use of their capability. Thus, having an appropriate scheduling and control on DGs is a crucial issue for distribution system operators. In this paper, a linear multi-objective model for power distribution system scheduling that coordinates tap-changers, photovoltaics (PVs) and battery energy storage operation is proposed. Accordingly, tap-changers experience lower stress, batteries' state of charge is kept in suitable range and DGs are used more effectively. The objective functions of the proposed model encompass improving voltage profile, minimizing losses and peak load. Epsilon-constraint method is employed for solving the multi-objective problem, generating the Pareto set. A new decision-making method is proposed to select the preferred solution from the Pareto set. The 33-bus IEEE test system is used to test the performance of the model. Conclusions are duly drawn.**

***Index Terms*—Linearization, Losses reduction, Multi objective, Peak power reduction, State of charge, Voltage control.**

I. NOMENCLATURE

A. Sets and indexes

i	Index of buses
$Slack$	Subset of i that refers to the slack Bus
PV	Buses with generating unit
t	Index of time (hours)
t_{Light}	Index of light load hours
t_{Heavy}	Index of heavy load hours
t_{Peak}	Index of peak load hours

B. Constants

S_{bat}	Battery`s capacity in power`s unit
$P_{\max}$	Inverter's maximum allowed active power in light load
$SoC_{\max}$	Maximum boundary of batteries state of charge
$SoC_{\min}$	Minimum boundary of batteries state of charge
$V_{\max}$	Maximum boundary of bus voltages
$V_{\min}$	Minimum boundary of bus voltages
S_{inv}	Inverter's capacity
$Q_{\max}$	Inverter's maximum allowed reactive power in heavy load
η_{inv}	Inverter's efficiency
η_C	Battery energy efficiency

C. Variables

A_{hbat_in}	Input ampere-hour to the battery
$Ah_{capacity}$	Battery capacity
$Ah_{delivered}$	Output Ampere-Hour from the battery
$V_i(t)$	Voltage of i^{th} bus at time t
f	Voltage deviation function
$Y_i(t)$	Auxiliary variable that linearizes voltage deviation function
$SoC(t)$	Batteries state of charge at time t
$P_{g_i}(t)$	Active power generation of i^{th} bus at time t
$P_{l_i}(t)$	Active load of i^{th} bus at time t
$P_{d_{i_{nom}}}$	Active load of i^{th} bus in voltage 1 p.u.
$P_{MMPT}(t)$	Maximum active power of the solar system
$P_{loss}(t)$	Grid losses at time t
$Q_{g_i}(t)$	Reactive power generation of i^{th} bus at time t
$Q_{l_i}(t)$	Reactive load of i^{th} bus at time t

Parts of the research leading to these results has received funding from the EU under the H2020 Framework Programme, GA no. 731148 (INVADE H2020 project). J.P.S. Catalão acknowledges the support by FEDER funds through COMPETE 2020 and by Portuguese funds through FCT, under Projects SAICT-PAC/0004/2015 - POCI-01-0145-FEDER-016434, POCI-01-0145-FEDER-006961, UID/EEA/50014/2013, UID/CEC/50021/2013, UID/EMS/00151/2013, 02/SAICT/2017 - POCI-01-0145-FEDER-029803, and also funding from the EU 7th Framework Programme FP7/2007-2013 under GA no. 309048.

II. INTRODUCTION

A. Motivation and Aim

Nowadays, renewable energies advantages are very important in decarbonization of the electric section. As a result, national and international policies have been conducted towards renewable energies increased shares. For instance, in 2005 only six countries were holding auctions to expand the use of renewable energy resources. However, this number reached to at least 67 countries at the end of 2016. Photovoltaic panels have a significant growth due to their technological progress and falling price. Their installed capacity increased from 40 GW in 2010 to 219 GW in 2015 and according to forecasts it will provide about 7% of global energy in 2030 [1]. In addition to DG, energy storage becomes an important issue. According to forecasts, the capacity of stationary energy storage will increase 10 times in 2025 compared to 2017 [2]. Since the presence of DGs and storage in the system can affect grid control, their coordination is of high importance. This work aims at proposing a strategy for dealing with this challenge.

B. Literature Overview

One of the current voltage control approaches is to determine optimum reference values of voltages in controllers of the network [3]-[4]. This means that, in each hour, the values of the control parameters are specified. These values in a specific time are applied to the controllers. In [5], a novel cooperative protocol has been proposed to deliver an appropriate voltage control for several feeders considering a transformer tap-changer, unbalanced load variety and several DG units in every feeder. Two conflicting objectives have been defined for each control agent. In [6], the capability of reactive power control and battery energy storage has been used. Since, the injection of power causes voltage rise, just in the required moments it uses reactive power and storage for voltage improvement.

In [7]-[8], a sensitivity analysis is used to identify an appropriate control action. In the online applications, the state estimation is used to determine the control parameters [9] and [10]. In [11], several different strategies have been presented for charging and discharging of batteries in the system. In [12], the distributed control by means of consensus algorithm adjusts feeder voltages within mandatory limits, while the localized control adjusts the state of charge (SoC) of each ESS inside the anticipated SoC range. In [13], an optimal battery management algorithm has been presented for the battery energy storage system using dynamic programming that will minimize output fluctuations. In [14], several control strategies have been used for the voltage regulators and addresses the likely impact that a smart transformer could bring on decreasing system voltage violations. A smart transformer, which includes a fixed tap transformer with a power-electronics voltage regulator, has the potential to lessen this problem by changing the line voltage in an automatic manner in responding to variations in loading. Network segmentation to various control areas based on the electrical distance between the voltage controllers prevents additional functionality of the equipment [15].

In [16], suitable values of active/reactive power are computed by dispatching. Then, these values are forwarded for a local channel controller by telecommunication links. In [17], a strategy has been presented for reactive power injection (or absorption) in voltage emergency situations.

It should be noted that distribution optimal power flow is a necessary tool for static voltage regulation. In [18] a comprehensive three phase DOPF is proposed that can be used for voltage regulation purposes. Also, voltage dependent modeling of customer loads increases model accuracy. Plug-in Electric Vehicles are an important component in smart distribution grids. In [19] a modeling framework for the analysis of PEV charging in unbalanced, residential distribution systems is proposed that can be used for coordination purposes.

C. Features and Novelties

In this work, voltage profile improvements, as well as reduction of losses and peak have been considered as the main objectives of coordinating voltage controllers. These aims will be achieved due to the voltage influence on the power of electrical loads and the use of energy storage in the network for power shifting. Accordingly, by using an appropriate planning at peak hours of consumption and choosing a suitable voltage level, the peak of load power will be reduced. In addition, energy storage improves the status of the network in peak hours by shifting production power injection from peak hours of production to peak hours of consumption. But, the appropriate and optimum use of storage is carried out by a constraint that provides their optimum usage that keeps the state of charge within a suitable range. Also, for increasing computational speed, the problem formulation is linearized.

III. PROPOSED VOLTAGE CONTROL CHARACTERIZATION

In Fig. 1, the connection diagram of a DG to the distribution network is shown. Clearly, the amount of power produced by DG affects the direction of power exchange between the network and DG. Obviously, in the direction that power flows, a voltage drop occurs due to the resistance and reactance. Equation (1) shows the approximate amount of this voltage drop [3].

$$\Delta V \approx \frac{RP_i + XQ_i}{V_i^*} \tag{1}$$

If V_i is considered as the reference voltage, i.e. 1 p.u,

$$\Delta V \approx RP_i + XQ_i \tag{2}$$

where $P_i = \pm P_{g_t} - P_{l_t}$ and $Q_i = \pm Q_{g_t} - Q_{l_t}$. According to the above formula, active and reactive powers of the DG are controlling factors in voltage regulation. However, since the main task of DGs is to generate active power, the priority is to maximize the utilization of generated power. By using the maximum power point tracking (MPPT) facility, the capacity of the DGs, e.g., PVs, is fully used. Nevertheless, this causes some problems; one is that during peak hours of radiation for PVs, a voltage rise occurs in the system and on the other hand the PV systems may not have production in peak hours, and due to high load conditions the network may experience severe voltage drops, while the voltage of buses should not violate the permitted boundary as given in (3) and (4):

$$V_i(t) \le V_{\max} \tag{3}$$

$$V_i(t) \ge V_{\min} \tag{4}$$

Battery is used as energy storage to fix this problem. Battery should be placed on the network so that it has no interference with the tap changer and active and reactive power of voltage controllers. Besides, their charging and discharging scheduling should be controlled.

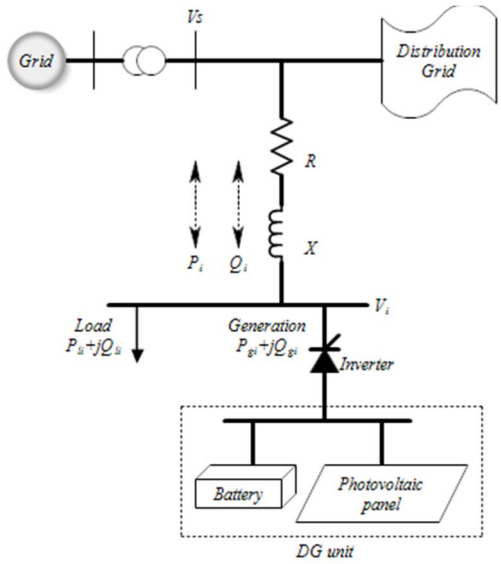

Figure 1. DG's Voltage regulation in PCC.

To this end, the SoC of batteries should be updated every time as follows:

$$Ah_{bat\_in} = \frac{P_{MPPT} - \left(\frac{P_g}{\eta_{inv}}\right)}{V} \times 1h \quad (5)$$

$$Ah_{Delivered} = Ah_{bat\_in} \times \eta_C \quad (6)$$

$$SoC(t) = SoC(t-1) + u \cdot \frac{Ah_{Delivered}}{Ah_{Capacity}} + (1-u) \cdot \frac{Ah_{bat\_in}}{Ah_{Capacity}} \quad (7)$$

$$Ah_{Delivered} \le u \cdot Ah_{bat\_in} \quad (8)$$

$$u = \{0,1\} \quad (9)$$

$$P_g(t) \le P_{MPPT}(t) + SoC(t) \cdot S_{bat} \quad (10)$$

$$\left(P_{g_i}(t) - P_{MPPT}(t)\right) \cdot \eta_c \le r.S_{bat} \quad (11)$$

$$P_{MPPT}(t) - P_{g_i}(t) \le r.S_{bat} \quad (12)$$

Equation 5 calculates input ampere-hour to the battery. The output ampere-hour of batteries that is lower than their input is shown in (6). Equation (7) shows the SoC, while (8) is written in such a way that sets u to 0 or 1, respectively, when the battery is being discharged or charged. Equation (10) shows the output power of the DG unit considered as a variable limited to MPPT and batteries SoC. Equations (11) and (12) limit the input or output ampere-hour to a fraction of batteries' capacity to prevent batteries from being damaged, where r is a constant between 0 and 1. To prevent inappropriate SoC, the following constraints are considered:

$$SoC(t) \le SoC_{\max} \quad (13)$$

$$SoC(t) \ge SoC_{\min} \quad (14)$$

The collection of batteries and photovoltaic sources are connected to the global network via the inverter. The inverter converts DC power to AC power with network frequency. It is noted that the operation of inverters is limited by some factors such as the capability curve of inverters, shown in Fig. 2.

$$S_{inv} = \sqrt{P_g^2 + Q_g^2} \quad (15)$$

Since Equation (15) is a non-linear equation, it will be linearized as it is shown in Fig. 3.

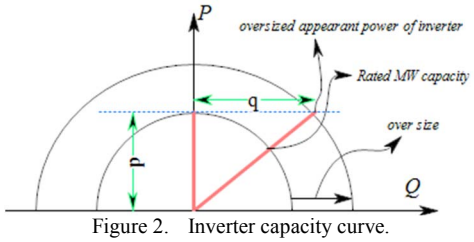

Figure 2. Inverter capacity curve.

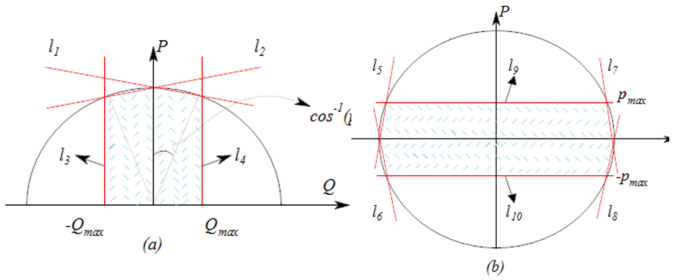

Figure 3. Linear Inverter capacity curve: (a). heavy load mode. (b). Light load mode.

Heavy load mode: The power factor of the inverter is limited to a lead-lag period that is close to 1. This limitation is done by considering the standards and local regulations. The inverter constraint will be changed as follows:

$$l_1(PV, t_{Heavy}) \le 0 \quad (16)$$

$$l_2(PV, t_{Heavy}) \le 0 \quad (17)$$

$$l_3(PV, t_{Heavy}) \ge 0 \quad (18)$$

$$l_4(PV, t_{Heavy}) \le 0 \quad (19)$$

Light load mode: Power generation can cause problems for the network in light load conditions. On the other hand, reactive power operation mode of the inverter helps the network to improve the situation. To this end:

$$l_5(PV, t_{Light}) \le 0 \quad (20)$$

$$l_6(PV, t_{Light}) \ge 0 \quad (21)$$

$$l_7(PV, t_{Light}) \le 0 \quad (22)$$

$$l_8(PV, t_{Light}) \ge 0 \quad (23)$$

$$l_9(PV, t_{Light}) \le 0 \quad (24)$$

$$l_{10}(PV, t_{Light}) \ge 0 \quad (25)$$

Another very important constraint that models the network corresponds to load flow equations. It should be noted that the tap-changer is modeled in load flow equations in the form of π model [20]. The employed linear load flow is proposed in [21]. The implemented load flow equations are as follows:

$$\begin{bmatrix} -A_r \\ -A_i \end{bmatrix} = \begin{bmatrix} B_r + C_r & B_i - C_i \\ B_i + C_i & -B_r + C_r \end{bmatrix} \cdot \begin{bmatrix} V_r \\ V_i \end{bmatrix} \quad (26)$$

$$A = Y_{NS} \cdot V_s - 2h \cdot S_{PN}^* + h \cdot S_{IN}^* \quad (27)$$

$$B = h^2 \cdot diag(S_{PN}^*) \quad (28)$$

$$C = Y_{NN} - h^2 \cdot diag(S_{ZN}^*) \quad (29)$$

where S_{PN}, S_{IN} and S_{ZN} are vectors of constant power, constant current and constant impedance loads. In [21], A, B and C are defined in detail.

$$Y_{bus} = \begin{bmatrix} Y_{SS} & Y_{SN} \\ Y_{NS} & Y_{NN} \end{bmatrix} \quad (30)$$

$$h=\frac{1}{V_{nom}} \overset{in\ p.u.\ system}{\underset{V_{nom}=1\ p.u.}{\Rightarrow}} h=1 \tag{31}$$

Minimization of Equation (32) causes the improvement of the network voltage profile.

$$f = \left|V_i(t)-1\right| \tag{32}$$

Equation (32) is a nonlinear function that contains absolute value. However, by defining an auxiliary positive variable y, it can be changed to a linear function, as follows:

$$\min y_i(t)$$
$$y_i(t) \geq V_i(t)-1,\ y_i(t) \geq 1-V_i(t),\ y_i(t) \geq 0 \tag{33}$$

The second objective function is related to the system's losses. Equation (34) shows losses through the line ij with impedance Z_{ij} and current $I_{ij}(t)$ at time t:

$$P_{loss}(t) = I_{ij}^2(t).Z_{ij} \tag{34}$$

Equation (35) indicates that the difference between total production and total consumption in a system is equal to the sum of system losses.

$$P_{loss}(t) = \sum_i P_{g_i}(t) - \sum_i P_{l_i}(t) \tag{35}$$

By reducing the voltage, the magnitude of these loads' current and power is reduced as well, as shown:

$$Z = V/I \tag{36}$$

where Z is the equivalent impedance of the load, and V, I and P are voltage, current and active power of the load, respectively. Constant current loads receive constant current from the source at any voltage. According to Equation (37), with the reduction of voltage, power reduces too:

$$P = V.I \tag{37}$$

To speed up the performance of the algorithms and also due to lack of access to all types of loads, a very important feature can be used that indicates that approximately with every 1% increase or decrease in the voltage, power increases or decreases 1% [22]. Thus, a linear relationship between power and voltage can be obtained:

$$P_{Peak} \approx P_0 \times V_{Slack} \tag{38}$$

$$P_0 = \sum P_{d_{inom}} \tag{39}$$

where P_{Peak} and V_{Slack} are the peak of power and voltage of the slack bus. Thus, the constraint related to reducing peak power is applied to the optimization problem in the form:

$$P(t_{Peak}) \approx P_0 \times V(Slack, t_{Peak}) \tag{40}$$

Generally, the decision variables are tap-changer position, P_i and Q_i that are related to the output power of PV, batteries SoC and output reactive power of the inverter.

IV. Multi-Objective Optimization and Decision Making

In a multi-objective optimization, the concept of a single optimal solution changes to a set of efficient solutions, i.e., a Pareto front (set). An efficient method for solving a multi-objective problem is the epsilon-constraint method [21]. The flowchart of the proposed method is shown in Fig. 4. In the epsilon-constraint method, an objective is selected as the main goal and the others are added to the problem as constraints. In this work the objective functions are:

$$f_1 = \sum_t \sum_i y_i(t),\quad f_2 = \sum_t P_{loss}(t),\quad f_3 = \sum_{t_{Peak}} P(t_{Peak})$$

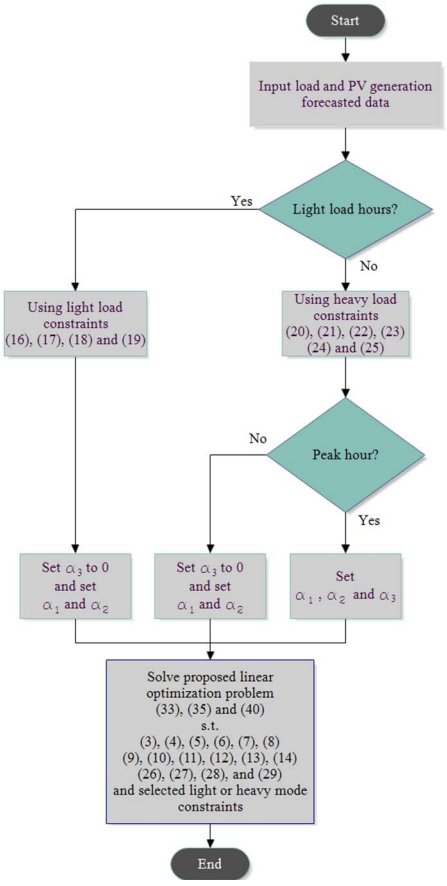

Figure 4. Flow-chart of the proposed model.

where f_1 is considered as the main objective and f_2 and f_3 are added to the problem as constraints. Accordingly, the multi objective formulation is as follows:

$$\textbf{min}\ f_1(\bar{X})\ \textbf{subject to}\ \ f_2(\bar{X}) \leq e_2, f_3(\bar{X}) \leq e_3 \tag{41}$$

$$e_2 = f_{2_{\min}} + \left(\frac{f_{2_{\max}} - f_{2_{\min}}}{q_2}\right).n_2,\ n_2 = 1,2,...,q \tag{42}$$

$$e_3 = f_{3_{\min}} + \left(\frac{f_{3_{\max}} - f_{3_{\min}}}{q_3}\right).n_3,\ n_3 = 1,2,...,q \tag{43}$$

where $\bar{X}$ refers to the decision variable, and $\bar{X}^*$ is the optimal solution. Also, $f_{i_{min}}$, $f_{i_{max}}$ are picked up from the payoff table in Equation (45) and q is the number of required iterations to generate the Pareto set.

$$\Phi = \begin{bmatrix} f_1^*(\bar{X}_1^*) & f_2(\bar{X}_1^*) & f_3(\bar{X}_1^*) \\ f_1(\bar{X}_2^*) & f_2^*(\bar{X}_2^*) & f_3(\bar{X}_2^*) \\ f_1(\bar{X}_3^*) & f_2(\bar{X}_3^*) & f_3^*(\bar{X}_3^*) \end{bmatrix} \tag{45}$$

Respectively $f_i^*(\bar{X}_i^*)$ and $f_j(\bar{X}_i^*)$ are the optimum values of f_i in the presence of the main constraints and the value of f_j in the point $\bar{X}_i^*$ that is the optimum point for f_i. So, minimum and maximum of ith row are considered as $f_{i_{\min}}$ and $f_{i_{\max}}$.

Details of the payoff table calculation can be found in [23]. As it is mentioned before, the selection of the best solution depends on the decision maker's judgment.

An appropriate method is proposed that helps to make better decisions. The selection of the best answer depends on decision maker's opinion. It can be done as a simple multi-objective optimization, such as (46):

$$\min(\alpha_1 f_1 + \alpha_2 f_2 + \alpha_3 f_3) \quad (46)$$

parameters α_1, α_2, and α_3 are the weights of different objective functions.

V. Numerical Results

Standard IEEE 33-bus network that can be seen in Fig. 5, has been considered to evaluate the performance of the proposed voltage control optimization framework. Reference voltage at all of the buses is 12.66 kV and reference power is 1 MVA. More information about this network is available in [24]. A 1.054MW PV power plant has been installed at bus 30. A 5MW battery unit is placed in bus 30 too. The profile of MPPT sun radiation has been considered for this plant as shown in Fig. 6.

Also, an oversize is considered in inverters capacity to support the network reactive power. Accordingly, an inverter has been selected with the capacity of 1.112MW. The 24-hour planning of the network determines the optimum points according to different objective functions. The independency of objective functions should be proven before running the optimization problem. For this purpose, the payoff table is formed as follows:

$$\Phi = \begin{bmatrix} f_1^*(\bar{X}_1^*) & f_2(\bar{X}_1^*) & f_3(\bar{X}_1^*) \\ f_1(\bar{X}_2^*) & f_2^*(\bar{X}_2^*) & f_3(\bar{X}_2^*) \\ f_1(\bar{X}_3^*) & f_2(\bar{X}_3^*) & f_3^*(\bar{X}_3^*) \end{bmatrix} = \begin{bmatrix} 8.975 & 3.745 & 1.378 \\ 13.459 & 3.653 & 1.548 \\ 24.234 & 3.654 & 1.258 \end{bmatrix}$$

In Fig. 7(a), functions of voltage deviation from base value and peak power are shown. By more focus on the peak reduction, the voltage deviation increases. In Fig. 7(b), voltage profile improvement and reduction of losses have been presented. When grid controllers are used to decrease the losses, voltage deviation increases. But, since these three functions have the same importance, they should be considered in multi-objective optimization, simultaneously. The collection of optimum answers has been computed to reduce all three objective functions, shown in Fig. 7(c).

In Fig. 8(a), the voltage profile has been shown at peak hour for different modes. Without DG, the main substation's tap-changer only acts as a controller for voltage regulation. Thus, in order to prevent voltage drop, the tap-changer fixes the voltage of the main substation to a maximum allowed value. PV installation improves the voltage profile in its generation hours.

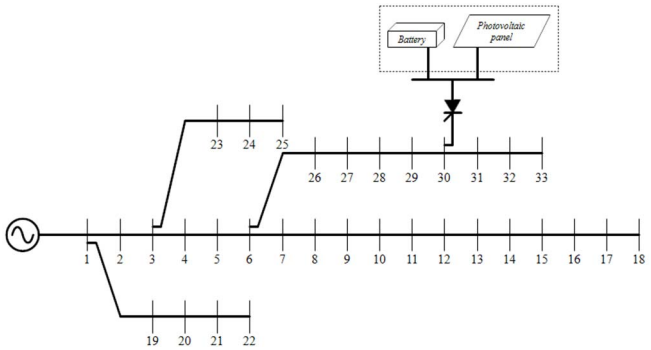

Figure 5. IEEE 33 bus test model.

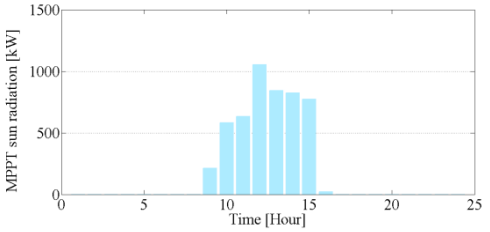

Figure 6. Profile of MPPT sun radiation.

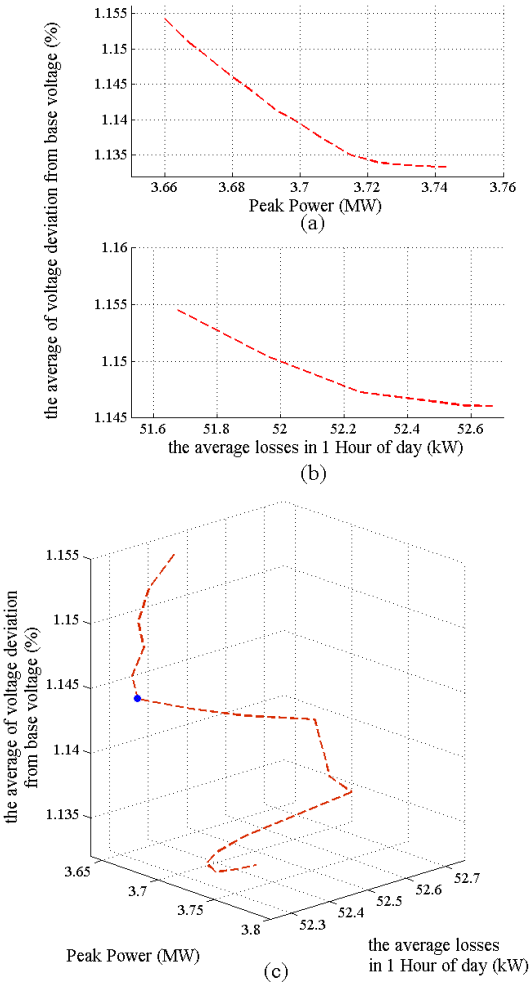

Figure 7. Multi-objective reference points: (a). Voltage deviation-Peak power, (b). Voltage deviation-average losses, (c). Voltage deviation-Peak power-average losses.

Also, in other hours such as peak hours, the voltage profile comes close to 1 p.u. due to the capacity of reactive power control. The presence of storage alongside PV causes a flatter voltage profile. The motive for this is that the active power injection to the grid enters the optimization problem as a decision variable. Finally, according to the best solution that minimizes voltage deviation, peak and losses simultaneously, the tap-changer decreases the voltage level in order to reduce the peak power.

In Fig. 8(b), the voltage of the main station has been shown at 24 hours. As it is clear, the tap changer is under less pressure in the presence of DG, the use of storage improves the condition of the system and tap changer works influentially.

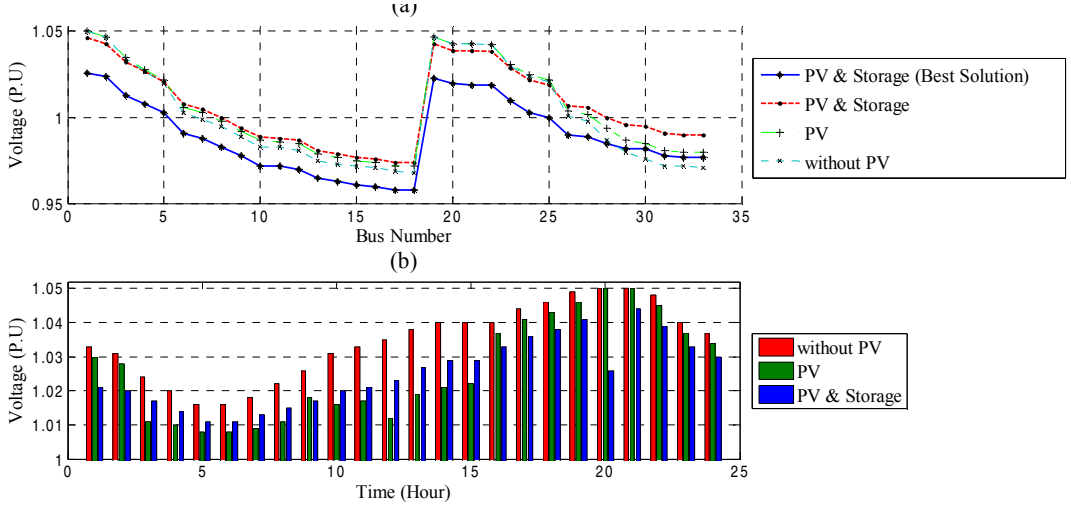

Figure 8. Voltage profile at peak hour: (a). 33 bus, (b). Slack bus.

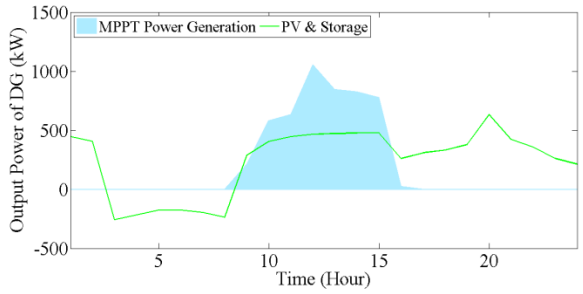

Figure 9. DG-grid power exchange.

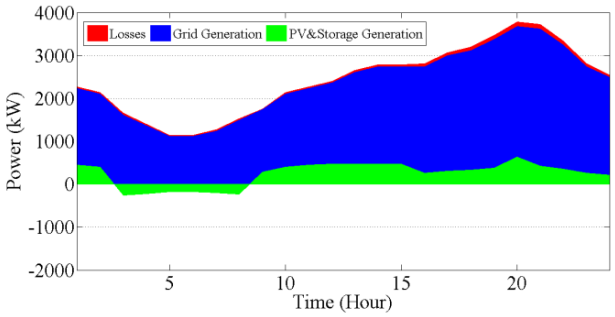

Figure 10. Forced power to grid.

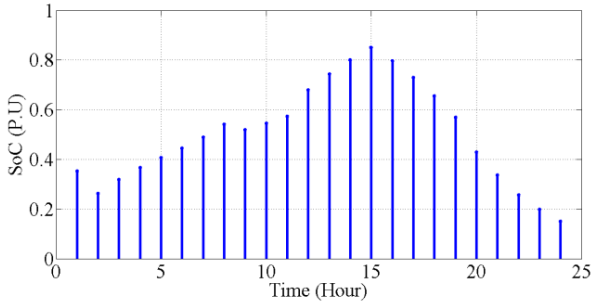

Figure 11. Battery SoC.

TABLE I. GRID LOSSES

	WITHOUT DG	DG	DG & Storage	Best Solution
Losses at peak load [kW]	146	155	118	106

In fact, the tap changer doesn't operate in non-preferred zones that are close to its limits. Also, observed network losses at peak hour under the different conditions have been reported in Table I. As can be seen, the use of DG increases the losses of the network. But, the use of storage with DG converts it to a dispatchable source and so, the losses will be reduced. With multi-objective optimization and appropriate decision making, both losses have been reduced and peak power has been decreased. Moreover, an appropriate voltage profile is produced. As mentioned, voltage affects peak power. Accordingly, the peak load of the network has been reduced from 3.715 MW to 3.682 MW. Another way to reduce peak power is using the storage and the injection from peak hours of production to peak hours of consumption. This power shift is shown in Fig. 9. Besides, another alternative method that can help network stability is the absorption of power by storage at low-load hours (e.g. at midnight). The green area in Fig. 10 shows that storage absorbs 1259kWh in these hours. In fact, it is located in the network as a load and prevents the low load of the network by charging the battery. Also, the amount of this power is injected into the network in needed situations. However, this absorption and injection operations don't hurt battery and the SoC of battery will be changed at the appropriate limitations. Fig. 11 shows that the battery SoC stays within 15 to 85% range.

VI. CONCLUSION

This paper proposed a strategy that coordinates the operation of grid's equipment for voltage control in distribution networks using a multi-objective optimization approach that concurrently minimizes network voltage deviation, peak load power and losses as objective functions. Linearizing inverter's capability curve is possible by dividing grid operation to heavy and light modes. Also, linearizing other constraints and using a linear distribution load flow speeds up the calculation. In addition, a decision-making process has been proposed to decide the best scheduling. The case study revealed a proper daily schedule, keeping battery SoC in allowable limits, preventing tap changers operation in non-preferred zones and providing a good employment of PVs, thus obtaining a suitable voltage profile with reduced peak and losses.

APPENDIX

Inverter capability curve linearizing is carried out by dividing its operation to heavy and light load modes that are shown in Fig. 3. In heavy load mode, because of having high consumption on the grid, the set of PV and battery firstly pays to active power supply, and then it activates the reactive power control ability. The range of its operation can be seen in Fig. 3(a). In these conditions the section of inverters capability curve that stays on operation range of heavy load mode can be linearized with lines l1 and l2. Also, l3 and l4 apply constraints of reactive power limitations. In the light load mode, the set of PV and battery works as an auxiliary service and has less emphasis on the injection of active power to the grid. So, as can be seen in Fig. 3(b) the power exchange between DG set and the grid is permitted in a limited range. Boundaries of operating limitations in the light load mode are approximated by l5 to l10.

$$l_1 = P - \left(\frac{S_{inv} - P(Q_{\max})}{-Q_{\max}} \right) \times Q - S_{inv}$$

$$l_2 = P - \left(\frac{S_{inv} - P(-Q_{\max})}{Q_{\max}} \right) \times Q - S_{inv}$$

$$l_3 = Q + Q_{\max} \qquad l_4 = Q - Q_{\max}$$

$$l_5 = P - \left(\frac{P_{\max}}{S_{inv} - \sqrt{S_{inv}{}^2 - P_{\max}^2}} \right) \times Q - \left(\frac{P_{\max}}{S_{inv} - \sqrt{S_{inv}{}^2 - P_{\max}^2}} \right) \times S_{inv}$$

$$l_6 = P + \left(\frac{P_{\max}}{S_{inv} - \sqrt{S_{inv}{}^2 - P_{\max}^2}} \right) \times Q + \left(\frac{P_{\max}}{S_{inv} - \sqrt{S_{inv}{}^2 - P_{\max}^2}} \right) \times S_{inv}$$

$$l_7 = P + \left(\frac{P_{\max}}{S_{inv} - \sqrt{S_{inv}{}^2 - P_{\max}^2}} \right) \times Q - \left(\frac{P_{\max}}{S_{inv} - \sqrt{S_{inv}{}^2 - P_{\max}^2}} \right) \times S_{inv}$$

$$l_8 = P - \left(\frac{P_{\max}}{S_{inv} - \sqrt{S_{inv}{}^2 - P_{\max}^2}} \right) \times Q + \left(\frac{P_{\max}}{S_{inv} - \sqrt{S_{inv}{}^2 - P_{\max}^2}} \right) \times S_{inv}$$

$$l_9 = P - P_{\max} \qquad l_{10} = P + P_{\max}$$

REFERENCES

[1] IRENA (2017), REthinking Energy 2017: *Accelerating the global energy transformation. International Renewable Energy Agency*, Abu Dhabi.

[2] IFC (2017), *Energy Storage Trends and Opportunities in Emerging Markets*. International Finance Corporation.

[3] Y. P. Agalgaonkar, B. C. Pal, R. A. Jabr, "Distribution voltage control considering the impact of PV generation of tap changers and autonomous regulators," *IEEE. Trans. Power Syst*., vol. 29, no. 1, pp. 182-192, 2014.

[4] Z. Ziadi, M. Oshiro, T. Senjyu, A. Yona, N. Urasaki, T. Funabashi, C. H. Kim; "Optimal Voltage Control Using Inverters Interfaced With PV Systems Considering Forecast Error in a Distribution System," *IEEE. Trans. Sustain. Energy*, vol. 5, no. 2, pp. 682-690, 2014.

[5] H. E. Z. Farag, E. F. El-Saadany, "A novel cooperative protocol for distributed voltage control in active distribution systems", *IEEE. Trans. Power. Syst*., vol. 28, no. 2, pp. 1645-1656, 2013.

[6] M. N. Kabir, Y. Mishra, G. Ledwich, Z. Y. Dong, K. P. Wong, "Coordinated control of grid connected photovoltaic reactive power and battery energy storage systems to improve to the voltage profile of a residential distribution feeder," *IEEE. Trans. Ind. Inf.*, Vol. 10, no. 2, pp. 967-977, 2014.

[7] V. Calderaro, G. Conio, V. Galdi, G. Massa, A. Piccolo, "Optimal decentralized voltage control for distribution systems with inverter-based distributed generators," *IEEE. Trans. Power. Syst*, vol. 29, no. 1, pp. 230-241, 2014.

[8] K. M. Muttaqi, A. D. T Le, M. Negnevitsky, G. Ledwich, "A coordinated voltage control approach for coordination of OLTC, voltage regulator, and DG to regulator voltage in a distribution feeder," *IEEE. Trans. Ind. Appl*., vol. 51, no. 2, pp. 1239-1248, 2015.

[9] D. Ranamuka, A. P. Agalgaonkar, K. M. Muttaqi, "Online voltage control in distribution systems with multiple voltage regulating devices," *IEEE. Trans. Sustain. Energy*, vol. 5, no. 2, pp. 617-628, 2014.

[10] S. N. Salih, P. Chen, "On coordinated control of OLTC and reactive power compensation for voltage regulation in distribution systems with wind power", *IEEE. Trans. Power. Syst.*, vol. 31, no. 5, pp. 4026-4035, 2016.

[11] J. V. Appen, T. Stetz, M. Braun, A. Schmiegel, "Local voltage control strategies for PV storage systems in distribution grids," *IEEE. Trans. Smart. Grid*, vol. 5, no. 2, pp. 1002-1009, 2014.

[12] Y. Wang, K. T. Tan, X. Y. Peng, P. L. S, "Coordinated control of distributed energy storage systems for voltage regulation in distribution network," *IEEE. Trans. Power. Del*, vol. 31, no. 3, pp. 1132-1141, 2016.

[13] S. A. Abdelrazek, S. Kamalasadan; "A weather based optimal storage management algorithm for PV capacity firming," *IEEE. Trans. Ind. Appl.*, vol. 52, no. 6, pp. 5175-5184, 2016

[14] J. D. Watson, N. R. Watson, B. Das, "Effectiveness of power electronic voltage regulators in the distribution network," *IET Gener. Transm. Distrib*. vol. 10, no. 15, pp. 3816-3823, 2016

[15] D. Ranamuka, A. P. Agalgaonkar, K. M. Muttaqi, "Online coordinated voltage control in distribution systems subjected to structural changes and DG availability", *IEEE. Trans. Smart. Grid*, vol. 7, no. 2, pp. 580-591, 2016

[16] A. M. García, R. A. Mastromauro, T. García-Sánchez, S. Pugliese, M. Liserre, S. Stasi, "Reactive power flow control for PV inverters voltage support in LV distribution networks," *IEEE. Trans. Smart. Grid*, vol. 8, no. 1, pp. 447-456, 2017.

[17] M. E. Baran, I. M. El-Markabi; "A multiagent-based dispatching scheme for distributed generators for voltage support on distribution feeders," *IEEE. Trans. Power. Syst*., vol. 22, no. 1, pp. 52-89, 2007.

[18] S. Paudyal, C. Cañizares, K. Bhattacharya; "Optimal Operation of Distribution Feeders in Smart Grids," *IEEE. Trans. Ind. Electronics*., vol. 58, no. 10, pp. 4495-4503, 2011.

[19] I. Sharma, C. Cañizares, K. Bhattacharya; "Smart Charging of PEVs Penetrating Into Residential Distribution Systems" *IEEE. Trans. Smart. Grid,* vol. 5, no. 3, pp. 1196-1209, 2014.

[20] Hadi Saadat, "Power System Analysis," *McGraw Hill*, USA. Third Edition. 2002.

[21] A. Garces, "A linear three-phase load flow for power distribution systems," *IEEE. Trans. Power. Syst*., vol. 31, no. 1, pp. 827-828, 2016.

[22] T. A. Short; "Electric power distribution handbook," ISBN: 0-8493-1791-6, CRC Press, 2004, section 5.3.4

[23] J. Aghaei, N. Amjady, H.A. Shayanfar, "Multi-objective electricity market clearing considering dynamic security by lexicographic optimization and augmented epsilon constraint method," *Appl. Soft Comp.*, vol. 11, no. 4, pp. 3846-3858, 2011.

[24] M. A. Kashem, V. Ganapathy, G.B. Jasmon, M.I. Buhari; "A novel method for loss minimization in distribution networks", in: *Proc. Int. Conf. Electric Utility Deregulation and Restructuring and Power Technologies – DRPT 2000*, London, UK, 2000.